43rd Turbomachinery & 30th Pump Users Symposia (Pump & Turbo 2014)
September 23-25, 2014 | Houston, TX | pumpturbo.tamu.edu

Honeycomb seal effect on rotor response to unbalance

Leonardo Baldassarre
Engineering Executive for Compressors, Expanders & Electrical Systems
General Electric Oil & Gas
Florence, Italy

Andrea Bernocchi
Senior Engineering Manager for Centrifugal Compressors
General Electric Oil & Gas
Florence, Italy

Leonardo Failli
Lead Design Engineer for Centrifugal Compressors
Upstream, Pipeline and Integrally Geared application
General Electric Oil & Gas
Florence, Italy

Michele Fontana
Engineering Manager for Centrifugal Compressors
Upstream, Pipeline and Integrally Geared applications
General Electric Oil & Gas
Florence, Italy

Nicola Mitaritonna
Lead Design Engineer for Centrifugal Compressors
New Product Introduction & Standardization
General Electric Oil & Gas
Florence, Italy

. **Emanuele Rizzo**
Senior Design Engineer for Centrifugal Compressors
New Product Introduction & Standardization
General Electric Oil & Gas
Florence, Italy

Leonardo Baldassarre is currently Engineering Executive Manager for Compressors and Auxiliary Systems with GE Oil & Gas, in Florence, Italy. He is responsible for requisition and standardization activities and for the design of new products for compressors, turboexpanders and auxiliary systems.
Dr. Baldassarre began his career with GE in 1997. He worked as Design Engineer, R&D Team Leader, Product Leader for centrifugal and axial compressors and Requisition Manager for centrifugal compressors.
Dr. Baldassarre received a B.S. degree (Mechanical Engineering, 1993) and Ph.D. degree (Mechanical Engineering / Turbomachinery Fluid Dynamics, 1998) from the University of Florence. He authored or coauthored 20+ technical papers, mostly in the area of fluid dynamic design, rotating stall and rotordynamics. He presently holds five patents.

Andrea Bernocchi is an engineering manager at GE Oil&Gas. He joined GE in 1996 as Centrifugal Compressor Design Engineer after an experience in plastic machinery industry. He has 18 years of experience in design development, production and operation of centrifugal compressor. He covered the role of LNG compressor design manager for 6 years with responsibility in design of LNG compressors, testing and supporting plant startup. He's currently leading the requisition team for centrifugal and axial compressor design.
Mr Bernocchi received a B.S. degree in Mechanical Engineering from University of Florence in 1994. He holds 4 patents in compressor field.

Leonardo Failli is currently a Design Engineer for Centrifugal Compressor Upstream, Pipeline and Integrally Geared Applications at GE Oil&Gas, in Florence, Italy. He is responsible to execute the calculation activities related to centrifugal compressor design and testing.
Mr. Failli graduated in Mechanical Engineering at University of Firenze in 2000. He joined GE in 2001 and moved as Centrifugal Compressor Design Engineer in 2010.

Michele Fontana is currently Engineering Manager for Centrifugal Compressor Upstream, Pipeline and Integrally Geared Applications at GE Oil&Gas, in Florence, Italy. He supervises the calculation activities related to centrifugal compressor design and testing, and has specialized in the areas of rotordynamic design and vibration data analysis.
Mr. Fontana graduated in Mechanical Engineering at University of Genova in 2001. He joined GE in 2004 as

Centrifugal Compressor Design Engineer, after an experience as Noise and Vibration Specialist in the automotive sector. He has co-authored six technical papers about rotordynamic analysis and vibration monitoring, and holds two patents in this same field.

Nicola Mitaritonna is a Lead design engineer in New Product Introduction for Centrifugal Compressors with GE Oil&Gas, Florence, Italy. His current duties are mainly focused on the rotordynamic design of new products. He has also worked for two years in the Oil&Gas test laboratory department. He has been working for GE in Oil&Gas business for 10 years.
Mr. Mitaritonna holds a M.S. degree in mechanical engineer from Georgia tech University 2009 and Politecnico di Bari 2003. Nicola also holds a post-graduate diploma course from Von Karman Institute for fluid-dynamics 2003.

Emanuele Rizzo is currently Senior Design Engineer in New Product Introduction for Centrifugal Compressors with GE Oil&Gas, Florence, Italy. His current duties are mainly focused on structural design, material selection and new applications of centrifugal compressors. Dr. Rizzo holds an MSc degree (Aerospace Engineering, 2003) and a Ph.D. degree (Aerospace Engineering, Conceptual Aircraft Design and Structural Design, 2007) from the University of Pisa (Italy). He joined GE Oil&Gas in 2008 as Lead Design Engineer in the centrifugal compressors requisition team, working mainly on high pressure compressors operating in sour environment. He has authored and coauthored several papers on aircraft design and optimization. He is co-inventor in two patents.

ABSTRACT

High pressure centrifugal compressors are often equipped with honeycomb seal on balance drum in order to optimize rotordynamic stability. In very high pressures applications (>200 bar) the direct stiffness and damping of the honeycomb seal may reach the same order of magnitude of the journal bearings, thus altering the peak frequency and amplification factor of rotor critical speeds as well as their mode shapes. This phenomenon is ultimately due to the density and viscosity of the gas leakage flowing through the seal, and it has a substantial effect on the rotordynamic behavior of the compressor.

According to current standards, aerodynamic seal effects are not necessarily included in the calculation of rotor response to unbalance. For high pressure compressors equipped with a honeycomb seal, the associated aerodynamic effects may have major impacts on rotor critical speeds in terms of frequency, amplitude and amplification factor. A procedure for the calculation of rotor response in loaded condition is here proposed, aiming to improve the predictability of the rotordynamic analysis and to provide practical criteria for the evaluation of the outcome.

A back-to-back compressor with final discharge pressure of 386 bar is presented as case study; it was tested at full pressure at Authors' Company facilities in 2013. In this case the stiffening effect of the honeycomb seal is particularly relevant, since it is positioned close to rotor midspan. Test measures show that in loaded condition the 1st critical speed shifts upwards by several thousand rpm, eventually exceeding the Maximum Critical Speed and even the Trip Speed of the compressor.

INTRODUCTION

High pressure centrifugal compressors are often equipped with honeycomb seal on balance drum, since its use in place of a classic labyrinth seal improves effectively the stability of the rotor while not yielding any significant impact in terms of layout, performance or reliability.

Rotordynamic instability is due to aerodynamic excitation, mainly generated by the gas circulating in the narrow annular cavities corresponding to rotor-stator seals. Physical models show how these destabilizing effects correspond to high cross-coupled terms of the stiffness matrix (k_{xy}), that have the overall effect of reducing the effective damping acting on the rotor. The knowledge of this mechanism might origin a misconception about how the honeycomb seal "works", i.e. that it would improve the stability of the rotor by adding little or no cross-coupled stiffness with respect to a standard labyrinth seal.

Test results carried out at OEM laboratories (Vannini et al., 2011) show the opposite: honeycomb seals are often associated to higher cross-coupled stiffness than the equivalent labyrinth seals; nonetheless, the overall stability is improved due to the direct stiffness and damping added by the honeycomb, that are much higher than for a traditional labyrinth. The small reduction of effective damping caused by k_{xy_HC} is overwhelmed by its large increase due to K_{xx_HC} and C_{xx_HC}. Overall, the effective stiffness K_{eff} and the effective damping C_{eff} are improved.

Honeycomb stiffness and damping are function of quite a large number of geometric and operating parameters, and in particular they strongly depend on the density of the gas flowing through the seal and on the pressure differential across it. They can be estimated with the aid of calculation codes such as Isotseal^{TM}, a tool based on a two-control-volume model developed by (Kleynhans and Childs, 1997), whose results have been experimentally confirmed (Childs and Wade, 2004).

For high pressure applications, K_{xx_HC} and C_{xx_HC} may reach values comparable to those of the journal bearings; in this case the honeycomb acts in some way as a third journal bearing, causing significant variations of the rotordynamic behavior: critical speed peaks are shifted upwards in frequency, while their amplification factor is usually reduced and the vibration amplitude at journal bearings decreases; mode shapes are changed; even the shaft centerline position is altered (Fulton and Baldassarre, 2007). Therefore a rotordynamic model that does not include honeycomb seal effects is representative of the

compressor operating at low or no load.

The first paper reporting experimental data relevant to the rotordynamic effect of a honeycomb seal is (Benckert and Wachter, 1980) and it was followed by more refined rotordynamic analyses that allowed to better evaluate the stiffness and damping associated to the honeycomb seal and their effect on rotordynamic stability, and to assess the influence of the clearance tapering (Childs, 1983; Nelson, 1984; Childs et al., 1989). Further experiences documented the effect of honeycomb seal on actual turbomachinery (Zeidan et al., 1993; Memmott, 1994; Gelin et al., 1997; Smalley et al., 2003).

These effects have been also experimentally verified by comparing radial vibration measured in mechanical running test under vacuum (no load conditions, zero honeycomb effects) and in full load test. *Figure 1* shows such a comparison for an existing high-pressure compressor, manufactured and tested by Authors' Company in 2007. In full load test conditions, at about 200bar(a) suction pressure, the first critical speed peak was shifted in frequency by more than 13%.

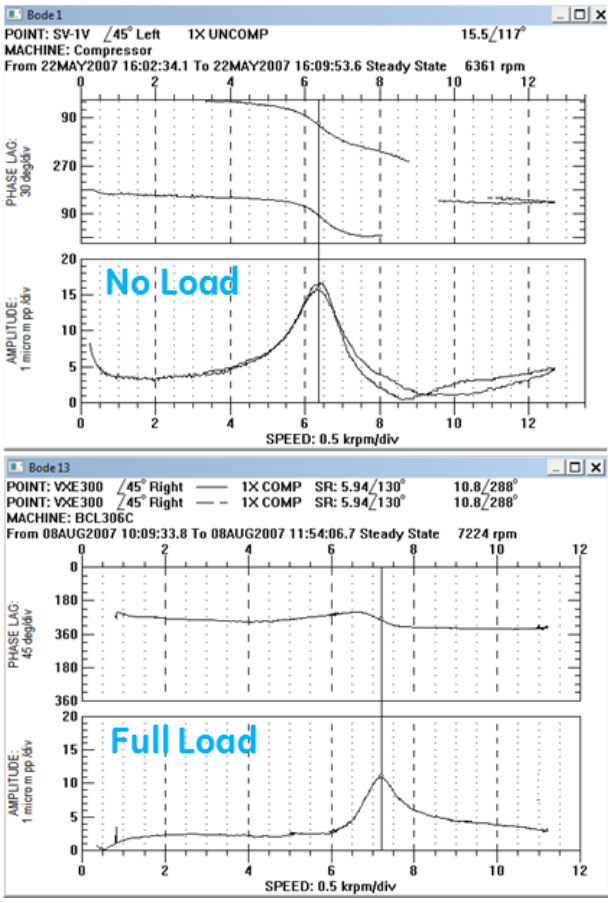

Figure 1. Bode plots of a high pressure centrifugal compressor. a) no load, b) full load.

Figure 2 represents another example of the effect of the honeycomb in high pressure compressors, showing the waterfall diagram of a compressor that is run at constant speed while increasing the load (i.e. pressurizing the gas loop). The upward shift of the first critical speed is clearly visible.

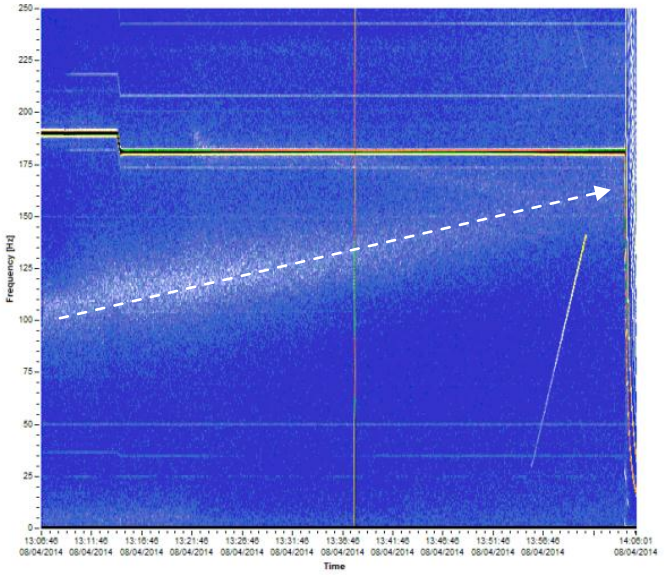

Figure 2. Waterfall diagram of a centrifugal compressor (type BCL306/C) equipped with honeycomb seal. The white, blurred band corresponding to the 1st critical speed peak is initially centered around 100Hz and the shifted up to ~150Hz when increasing the load.

An analysis of this topic was performed, focusing on the following main steps:

- Development of a reliable calculation model for the rotor response to unbalance in loaded conditions, including the honeycomb seal effects.
- Validation of the model through comparison with experimental data.
- Formulation of a general procedure for this rotordynamic analysis, derived from the standard guidelines for response to unbalance calculation provided in (API617, 2002). The application of the calculation model is not straightforward; some further assumptions are needed, as well as the selection of set of boundary conditions as representative of the general behavior of the compressor.
- Proposal of specific acceptance criteria, consisting in a generalization of API617 approach to response to unbalance calculation without aerodynamic effects.

THEORETICAL MODEL

Rotordynamics deals with the resolution of the dynamics of a rotor in the sense that natural mode shapes and frequencies are calculated. Moreover, in order to estimate the maximum deflection of the rotor, the effect of a periodic external load (unbalance) is applied in the maximum effect position, depending on the mode shape. Finally a stability analysis is carried out (API617, 2002).

The rotor is modeled by a finite elements scheme, including all the elastic and geometrical properties of each component. The model includes the rotor itself (i.e. shaft, impellers, coupling, sleeves, and so on) and the supports. In a rotor

equipped with oil bearings, the damping coming from the material internal friction is neglected since it is several orders of magnitude lower than the oil bearing damping. In this respect, the schematization depicted in *Figure 3* is employed.

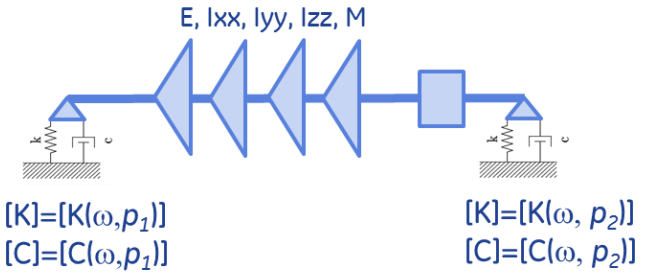

Figure 3. Schematization of rotor + journal bearings. Statically determined system

It is assumed that there are not significant variations in the geometry so that the inertial tensor [***I***] is constant. The only frequency (or speed) dependent quantities are the stiffness and the damping matrices of journal bearings. Moreover, these matrices are function of the static load *p* on the bearing itself. In a statically determined system, as the one depicted in *Figure 3*, the support reactions are constant, since they are not functions of the system stiffness. This is the typical case of, for example, the API617 mechanical running test (MRT).

The more general case of overconstrained system is depicted schematically in the *Figure 4*. The reactions at each support are functions of the system stiffness, each seal being a support that can be modeled by stiffness and damping matrices. Seal and honeycomb dynamic characteristics are function of speed and thermodynamic conditions but only slightly of static eccentricity (or, which is the same, of static load).

In general, seal eccentricity plays also a role in the frequency dependency of the seal dynamic coefficients. However, this dependency can be considered negligible provided that the maximum relative eccentricity is lower than 50% (Nielsen at al., 2012; Weatherwax and Childs, 2002; Weatherwax and Childs, 2003).

Moreover, preliminary results of tests carried out on honeycomb seal by author's company, seem to indicate that even at high pressures (~100 bar) the dependence of seal dynamic coefficient with static offset is negligible.

Bearing characteristics, on the contrary, are dependent on static load. Moreover stiffness and damping coefficient of bearing and labyrinth seals are almost non-frequency dependent (and usually are taken constant and equal to the synchronous value) while honeycomb shows strongly frequency dependent characteristics. It is worth noticing that in case of a honeycomb seal, the stiffness and damping matrices are also function of the rotor-stator gap and of its shape (tapering), in turn, is a function of speed, pressure and temperature surrounding it.

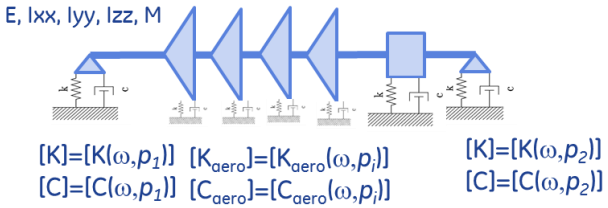

Figure 4. Schematization of rotor + journal bearings + honeycomb seal. Overconstrained system

Simplified approach

A first estimation of the AF and of the SM of the 1st forward mode in loaded conditions can be obtained by the results of standard level II stability analysis as per API617.
In particular:

- the amplification factor can be estimated by π/δ where δ is the calculated logarithmic decrement in loaded conditions;
- the separation margin is derived from the difference between the mode frequency in loaded conditions and the operative speed range.

The approximation of this simplified approach is generally acceptable for an estimation of the response to unbalance under loaded conditions.
More precise results can be obtained by the approach presented in the next paragraphs; for a comparison of the two approaches on an existing project see Table 1.

Condition	**1st Forward Mode**	
SURGE MCS	**AF**	**Frequency (cpm)**
No Load	8.03	7050
Load, simplified approach (Lev II results)	3.05	9190
Load, FPU Analysis	3.56	9500

Table 1. Comparison between results of simplified approach and complete analysis for an in-line high pressure compressor (Psuc = 60 bar ; Pdel = 180 bar)

Complete analysis

The first step for solving the complete rotordynamic problem is the solution of static case. Figure 5 below shows a flow chart summarizing the procedure for solving the static case.

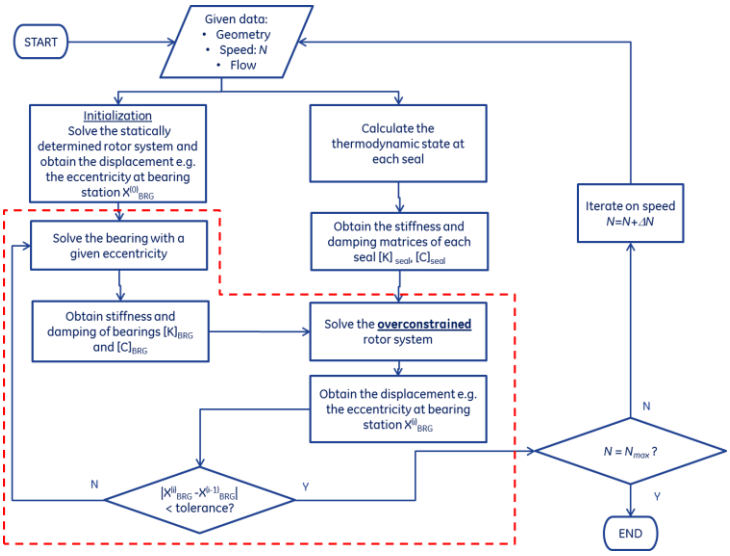

Figure 5. Static solution of the rotordynamic model. Since the bearing constitutive equation is not linear in the displacements, a Newton-Raphson solver scheme has been employed for the blocks in the red dashed envelope

Given the geometry, the rotational speed and the flow characteristics, the procedure consists of the following steps:

1. Assume the displacements along the two directions (horizontal and vertical) at bearing locations X_0
2. Solve the bearing with given eccentricity. As output the reactions (p) at bearings are calculated.
3. Calculate the bearing direct stiffness as $K_{brg} = p/X_{brg}$
4. From the seal module, calculate the stiffness matrix of seals K_{seal}
5. Solve the overconstrained problem and obtain the displacements at bearing locations X_1
6. If $| X_0 - X_1|$ < tolerance then convergence is reached; update the speed value and go to step 1, until all the speeds have been explored. Otherwise update X_0 and go to step 2.

Since the constitutive law for the bearing (e.g. the force-displacement law) is not linear, a Newton-Raphson procedure is used to solve iteratively the problem in the four bearing displacement unknowns (the update rule in STEP 6). In the above procedure, stiffness and damping matrices of labyrinth seals and bearings are considered constant with frequency and equal to the synchronous values, while honeycomb seal characteristics are frequency dependent[1].

The dependence of the honeycomb dynamic characteristics with frequency leads to follow a special procedure for the construction of the Campbell diagram.

Campbell diagram procedure:

1. Initialization: $i=2$
2. Divide the frequency range into a number of intervals sufficiently small to assume that the values of stiffness and damping are constant in that interval
3. Calculate the central frequency at the given interval $\bar{f}_i = \dfrac{f_i + f_{i-1}}{2}$
4. Calculate the honeycomb stiffness and damping matrices $K_{HC}\left(\bar{f}_i\right)$ and $C_{HC}\left(\bar{f}_i\right)$
5. Calculate modes and frequency of the rotor with all supports
6. Record the mode with frequency belonging to the interval $\left[f_i; f_{i-1}\right]$. Record also its logarithmic decrement.
7. Set $i=i+1$, repeat steps 3-7 until the maximum frequency is reached
8. Plot the recorded frequencies and logarithmic decrements as function of the speed

Such a procedure is needed because of the frequency dependence of the honeycomb characteristics. In case of only labyrinth and bearings, Campbell diagram can be constructed in a single run since synchronously reduced bearing coefficients have been used.

The procedure of Figure 5 shall be repeated at each thermodynamic state or, in other words, at each compressor operating point. Indeed, for example, if a start-up sequence is simulated, in order to have the thermodynamic state at each seal station the load sequence shall be known or assumed.

Figure 6 shows a typical operative envelope (map) of a centrifugal compressor (pressure ratio vs. volumetric flow as a function of speed). A starting sequence from 0 rpm to maximum continuous speed can be done along any pressure-flow-speed path inside the map, depending on the circuit characteristic curve. As limit cases, the yellow dots represent a hypothetical ramp-up done along the surge line, whereas the red dots represent a ramp-up done along the choke line.

1 The flow in the honeycomb seal is a function of the stator-rotor gap shape (tapering). Therefore stiffness and damping matrices are also functions of the local geometry that, in turns, is a function of temperature and pressure. The presented flowchart assumes a given, constant tapering. A more general and complete analysis would include the calculation of deflections of honeycomb seal and the analysis of the gap shape leading to complicate modelling. This can be overcome by repeating the procedure at given tapering values. Additionally, considerations on the seal eccentricity should be done in case of high eccentricity ratios (>50%).

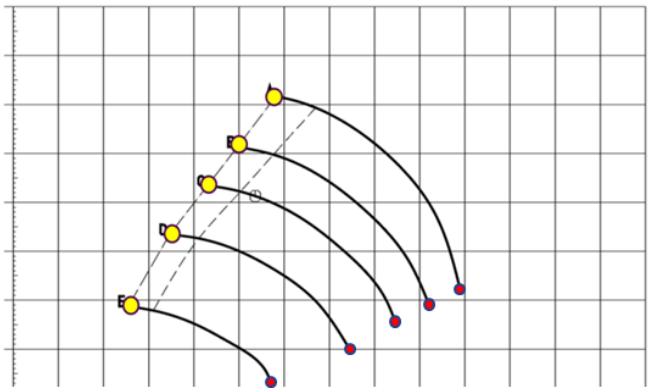

Figure 6. Centrifugal compressor map.

As extreme case analysis, a ramp-up along surge with the highest molecular weight and a ramp-up along choke with the lightest molecular weight can be assumed, being all other cases included into these two extreme cases.

The procedure shown above has been applied to a back-to-back centrifugal compressor and results have been compared with the full load test carried out at author's shop.

BACK-TO-BACK COMPRESSOR DESCRIPTION AND ROTORDYNAMIC MODEL

Case Study

The above procedure has been applied to a back-to-back compressor equipped with honeycomb seal as center seal and results are compared with test readings acquired during a full load test made at OEM factory. A cross section of compressor is depicted in *Figure 7*. *Table 2* collects some compressor's data.

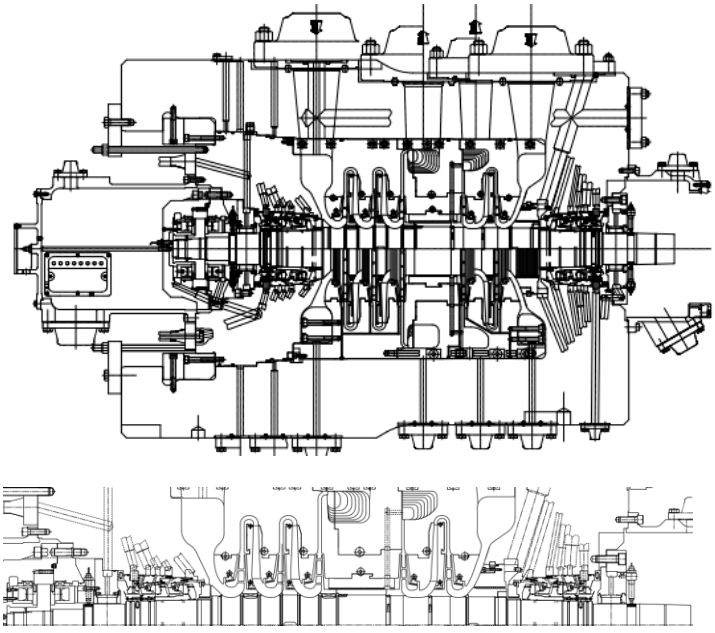

Figure 7. a) Centrifugal compressor cross section. b) Rotor detail

Compressor Configuration	Back to Back
Process Gas	Nitrogen
Compression Stages #	5 (3+2)
Operating speed range (rpm)	7604-11408
Journal bearing type	Tilting pad
Journal bearing nominal diameter (mm)	120
Coupling(s) size (mm)	120
Bearing span (mm)	1420
Rotor length (mm)	1928
Rotor total mass (kg)	450
Suction Pressure (barA)	110
Discharge Pressure (barA)	330

Table 2: Main Compressor data

Figure 8 shows the speed and pressures at four flanges as a function of time considered in the present simulation for which all experimental data are available.

The maximum achieved pressure is 330 bar(g), with a differential pressure across the interstage balance drum (where honeycomb is located) of about 110 bar. The suction pressure is 110 bar(g) at regime, SOP is 146 bar(g).

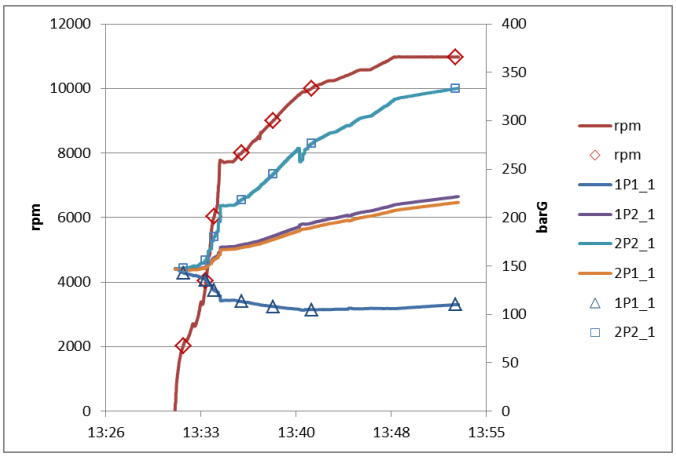

Figure 8. Readings during full load test used for the FPU analysis.

The dots in Figure 8 represent the thermodynamic states where the compressor performances and the seal coefficients have been calculated.

The rotor model is depicted in *Figure 9*.

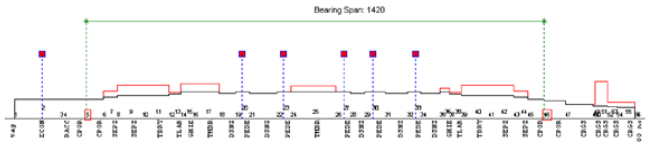

Figure 9. Rotor model of 2BCL505/C centrifugal compressor.

Standard API617 analysis (no load response to unbalance)

API617 requires performing an unbalance analysis for the system rotor plus bearing without any contribution of the seals. *Figure 10* below shows the results of such analysis for the case

under study for a 4*U* unbalance (~1000 g*mm, where *U*= 6350 *W*/*N*) placed in the middle of the rotor. The location of the unbalance is chosen to excite the first mode. Here station 5 and 46 are the bearing locations whereas station 25 is the middle of the rotor where the interstage balance drum equipped with HC seal is located. *Figure 11* shows the Bode plot recorded during MRT. *Figure 12* shows the relative Campbell diagram where the only contribution of the bearings is considered. The resonance at the critical speed is around 6900 RPM and an amplification factor of 4.8 (log dec of 0.64) is calculated. Predicted critical speed is in good agreement with measured critical speed and the measured AF is about 5.

The Campbell diagram clearly shows the second mode is well above the operational envelope of the machine. In the Campbell diagram blue stars represent the frequencies of each mode, and logarithmic decrement is reported in red text when it is less than 1.3, in black when it is between 1.3 and 2.5; it is not reported for values above 2.5.

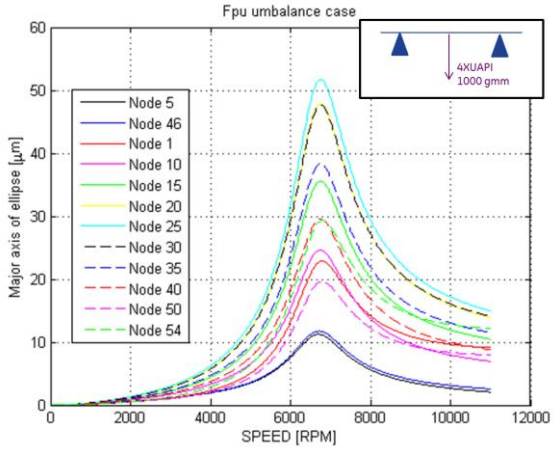

Figure 10. API617 response to unbalance.

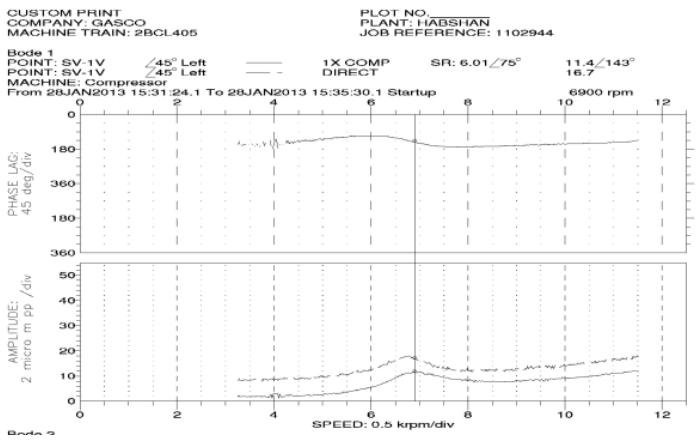

Figure 11. Experimental Bode plot recorded during MRT

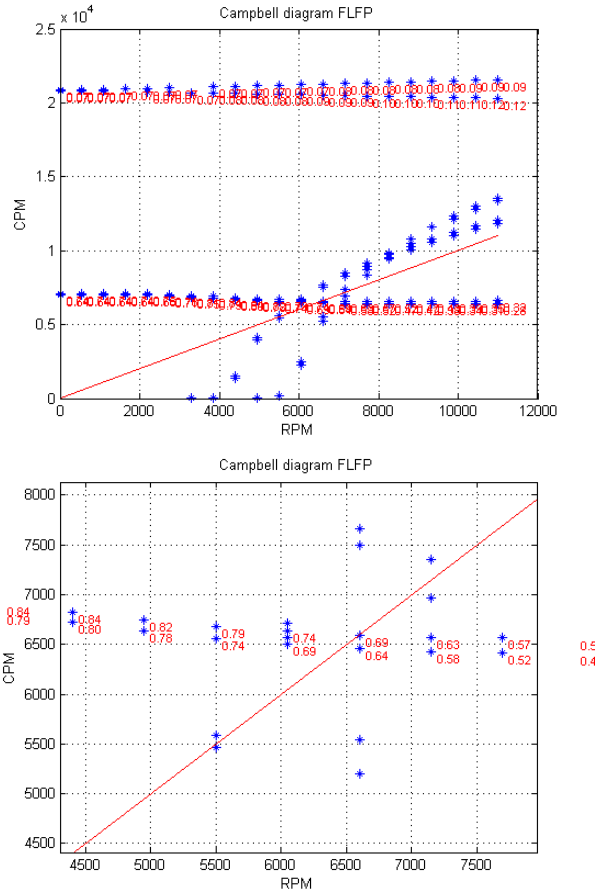

Figure 12. Campbell diagram (only bearings). a) full range Campbell diagram. b) zoomed area close to the 1st critical speed.

Full load response to unbalance

A full pressure unbalance (FPU) analysis as described above is carried out imposing a 4**U* unbalance weight at the maximum deflection point of the unloaded first mode and taking into account all the stiffness and damping matrices of all seals (this is an approximation since the mode shape changes as the stiffness of the system changes, so, in principle, the maximum deflection point in a given condition moves as operating point changes).

Figure 13 shows the Campbell diagram with aerodynamic effects of the rotor under study. Blue stars represent the frequencies of the modes. Logarithmic decrement is reported in red text if it is less than 1.3, in dark if it is between 1.3 and 2.5, and it is not reported for values above 2.5. It is worth noticing how after a certain speed (around 7000 rpm) the frequency of the first mode starts to increase and it follows the 1Xrev. This is due to the fact that the increasing pressure ratio across the honeycomb starts to increase its stiffness. Honeycomb is located at the center of the rotor so it is starting to act as a third bearing stiffening the system. This effect is known as "speed tracking" (API684). No effect is recorded on the second flexional mode (the one with low log dec) since this mode has a node in the center of the rotor. Now the critical speed of the rotor is not definable and, in fact, vibrations always increase

with speed without peaking (*Figure 14*).

The same behavior has been observed during the full load test as depicted in *Figure 15*, where the critical speed is not clearly defined.

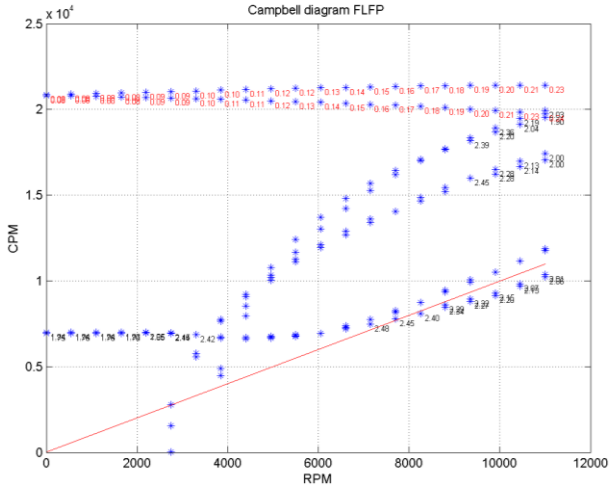

Figure 13. Campbell diagram for the full iterative solution (variable load on journal bearings, depending on honeycomb seal coefficients).

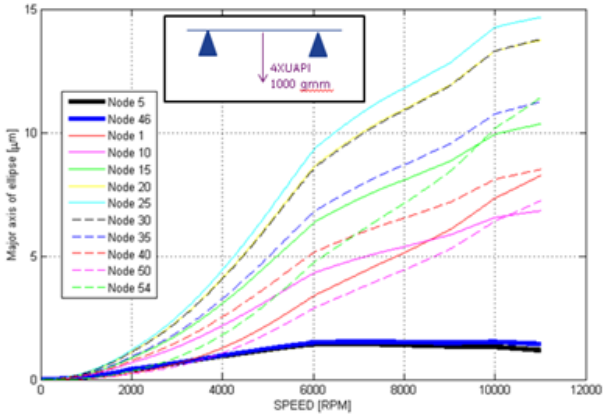

Figure 14. Full pressure response to unbalance plot, for first mode rotor unbalance

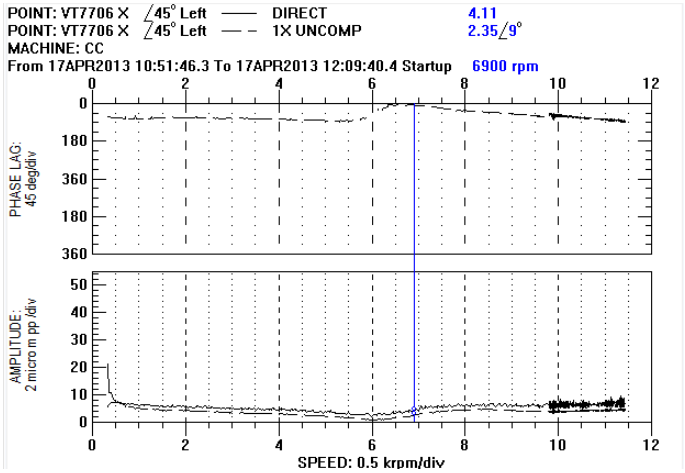

Figure 15. Vibration measurement (Bode plot) during full load test

By comparing *Figure 11* and *Figure 15* it can be inferred how at the same speed, the measured peak-to-peak vibration goes from 16.7 micron of MRT case to 4.1 micronsof full load test, being the ratio between no load vibration and loaded vibration 0.25.

It is worth noticing that now the system is much more stiff and able to withstand large unbalances. To enforce this concept, *Figure 16* below shows the comparison of the deformed shape of the rotor under the same unbalances at the critical speed for the predicted no load and loaded case. The vibration level considering the seal's contribution is three times less by comparing *Figure 10* and *Figure 14*.

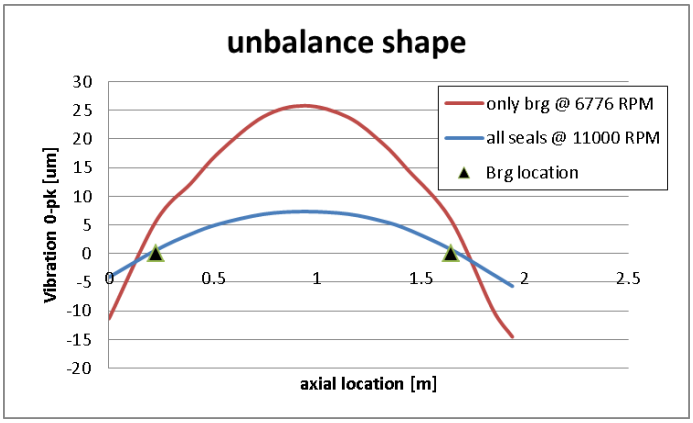

Figure 16. Comparison of half peak vibration of 1st mode between no-load and loaded conditions

Campbell diagram above, in *Figure 13*, has been constructed following the procedure described in previous section. In particular, the static equilibrium iterative procedure has been followed. Such procedure, anyhow, is very complicated and it can discourage the design engineer.

For this reason an attempt has been done to skip the iterative procedure and to consider the load on the bearing constant and equal to the one from simply supported rotor. Campbell diagram below in *Figure 17* shows the results. It is clear, comparing *Figure 13* and *Figure 17*, that the iterative procedure can be avoided where the contribution of the honeycomb is predominant as generally is the case in high pressure compressors. However, in a more general case if the eccentricity ratio is very high, a dependency of the seal dynamic coefficients with local displacements (e.g. local eccentricity) shall be taken into account by iterating also on the seal reactions. This is not the case for the present analysis, since both the tolerances on concentricity and the peak-to-peak vibrations are small compared to the seal clearances. This assumption is confirmed also by the good matching between prediction and test.

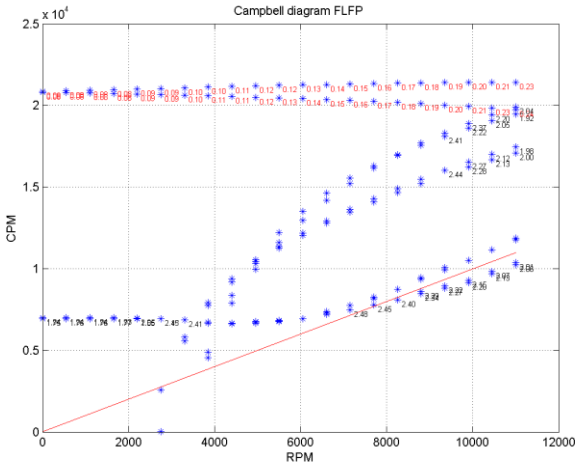

Figure 17. Campbell diagram for the simplified solution (fixed load on journal bearings, independent from honeycomb seal coefficients).

IMPLICATIONS FOR THE END USER

Due to the strong alterations caused by the honeycomb seal on the response to unbalance of high pressure compressors, the ordinary acceptance criteria for rotordynamic design (based on Separation Margin and Amplification Factor calculated without seal effects) may be not sufficiently accurate to assess the rotordynamic behavior in load conditions. On the other hand, the direct extension of API617 criteria to all possible operating conditions (inlet gas conditions, speed, flow rate) would be excessively conservative and often impossible to fulfill, besides generating an unnecessary and confusing amount of calculations and results. The purpose of the Authors was therefore:

1. to define the subset of centrifugal compressor applications where the inclusion of aerodynamic effects in the calculation of response to unbalance yields a significant improvement in predictability over the traditional API617 approach.
2. to propose a specific calculation procedure for the above identified cases.
3. to update the relevant acceptance criteria.

1. Applicability

Compressors equipped with honeycomb seal, for which the pressure differential across the seal evaluated at normal operating point is higher than 100bar (for in-line arrangements) or 50bar (for back-to-back arrangements, with honeycomb seal on the interstage balance drum) and the 1st forward mode calculated by API617 Level II approach yields a not satisfactory separation margin.

The procedure is referred only to response to unbalance across 1st critical speed. For high pressure compressors, higher critical speeds are typically outside the operating speed range and therefore not addressed by this study, although in principle the same approach can be extended to them.

2. Calculation Procedure:

2.1 Select case A as the most critical operating case on datasheet, according to the following criteria: highest gas molecular weight, highest discharge pressure at MCS & surge limit

2.2 Select case B as the least critical operating case on datasheet: lowest gas molecular weight, lowest discharge pressure at MCS & choke limit.

2.3 For case A trace a run-up ramp from zero to MCS that crosses each operating speed at the surge limit (yellow dots in *Figure 6*), and calculate the thermodynamic parameters of the compressor in at least 6 points across the ramp, in the speed range between 1st critical speed at no load and MCS.

2.4 For each point identified at previous step, apply the procedure depicted in the *Figure 5*. It is not necessary to iterate on the bearing displacements since the impact on results is negligible as shown in *Figure 17*. Assumptions about the honeycomb tapering shall be done for each point, for example by considering a constant value along the load path.

2.5 Plot the vibration amplitude vs. speed at the following rotor stations: DE and NDE radial vibration probe locations, labyrinth and honeycomb seal locations, coupling hub(s) location. Use these diagrams to calculate the 1st critical speed peak frequency, amplitude and AF.

2.6 Repeat steps 2.3 to 2.5 for case B.

As an additional note, most compression trains are started up in recycle, and then throttled to the design point by the closing of the recycle valve. This would make Case B more common.

3. Acceptance Criteria:

For high pressure compressors the inclusion of honeycomb seal aerodynamic effects in the calculation model may shift the 1st critical speed peak frequency by several thousand rpm. This means that in most cases it is materially impossible to have the Separation Margin requirement (defined as per API617) fulfilled over the specified operating speed range for both full load and no load conditions, as well as for all the possible intermediate operating conditions. It may happen that the $CS1_{FL}$ is close to or higher than $CS2_{NL}$, thus leaving no speed value between 1st and 2nd critical speed absolutely free from intersections.

The above considerations suggest that the ordinary acceptance criteria based on Separation Margin cannot simply be extended to the full load case. In order to define an optimized rule, it is helpful to review the evolution of the acceptance criteria defined by API, as referred mainly in (Nicholas, 1989):

- Originally API617 (up to 4th ed.) prohibited rotor operation on or near any critical speed, regardless of its amplification factor, defining a required minimum distance (separation margin) between the critical speed peak and the operating speed range.
- Since 5th edition, the requirement of a minimum separation

margin was lifted in the case of very damped critical speed peaks: *"If the amplification factor is less than 2.5, the response is considered critically damped and no separation margin is required"*.

- A further concession was introduced, specifying that *"If the analysis indicates that the SMs still cannot be met or that a non-critically damped response peak falls within the operating speed range and the purchaser and vendor have agreed that all practical design efforts have been exhausted, then acceptable amplitudes shall be mutually agreed upon by the purchaser and the vendor, subject to the requirement [that] the calculated unbalanced peak-to-peak rotor amplitudes […] shall not exceed 75% of the minimum design diametral running clearances throughout the machine"*.

The spirit of this concession is in line with the main concern of having critical speeds within the operating speed range of a rotating machine, which is the high vibration amplitude associated to resonance condition; it could possibly lead to malfunctioning and damage (rotor-stator rubbing). Even the definition of overdamped critical speeds is based on the same philosophy: the amplification factor is in some way a measure of the peak vibration amplitude with respect to the amplitude away from the critical speed; therefore a low AF (<2.5) is considered not "dangerous" for compressor integrity even in continuous operation.

API617 criteria may incur in the following objection:

Is it redundant to impose limits on the amplification factor and separation margin? The same standard already provides a limit for maximum vibration amplitude A *within the operating speed range (API617, Ch.1, 2.6.8.8), that has to be verified during mechanical running test. If a rotor has maximum vibration amplitude* A_{max}<A and *an undamped critical speed in the operating speed range, does it represent a concern?*

The answer is that, even if $A_{max}<A$, an undamped CS peak within the operating speed range has some residual criticality, since its amplitude is very sensitive to changes in operating parameters.

For a given exciting force with modulus F_0, the vibration amplitude is directly proportional to the amplification factor, that in turn is function of the damping ratio ζ:

$$\zeta = \frac{c_s}{2m\omega_n} \quad (1)$$

$$AF = \frac{1}{2\zeta} \quad (2)$$

$$A = \frac{F_0}{k} AF \quad (3)$$

The damping ratio is determined by the stiffness and damping coefficients of the system, which can be altered for example by changing the viscosity of the bearing lube oil, or the journal bearing clearance. Figure 18 shows that the AF sensitivity to ζ is very strong in the high-AF zone, while it is almost negligible when AF is low. This diagram makes clear the rationale behind selecting a threshold value for AF: for a sufficiently low amplification factor, any small variation of stiffness and damping due to operating parameters (lube oil temperature, journal bearing clearance...) or to inaccuracy in the input data used for calculations has a negligible effect on the peak amplitude. For example, reducing ζ by 0.01 at AF=2.5 would increase the peak amplitude by 5%, while applying the same variation at AF=5 and 10 would increase it by 11% and 25% respectively.

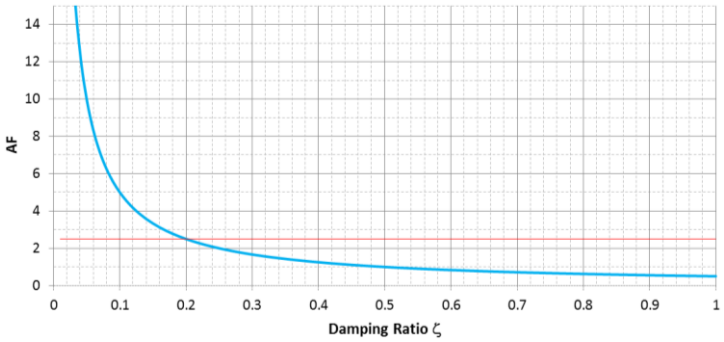

Figure 18. Amplification Factor as a function of damping ratio ζ.

The API617 criterion of requiring a minimum separation margin between the operating speed range and the critical speeds with AF ≥ 2.5 is therefore ultimately related to the vibration amplitude; this is also clear from subsequent point

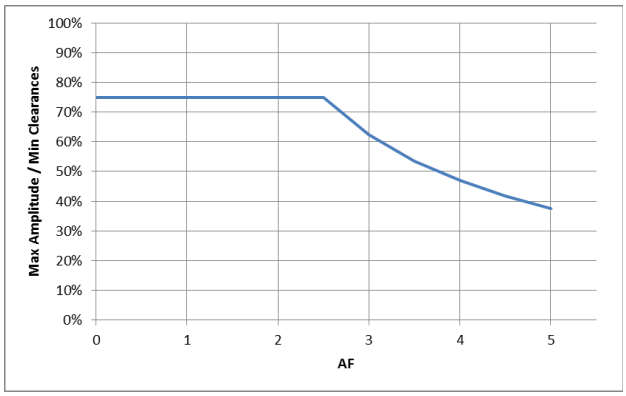

2.6.2.13 ("*...acceptable amplitudes shall be mutually agreed upon by the purchaser and the vendor...*").

Operating on or near to a critical speed may be completely acceptable or unacceptable, depending on rotordynamic considerations. Defining a threshold value for AF is a reasonable but partial approach, since it differentiates critical speed peaks basing on their shape but fails to take into consideration their amplitude. Since one main effect of the honeycomb seal is to strongly reduce the peak amplitude at seal locations, the acceptance criterion could be tuned to include also this aspect.

The current API617 acceptance criterion for response to unbalance is taken as reference, i.e.:

- a minimum separation margin between critical speed peaks and compressor operating speed range is required, unless

the amplification factor of the peak is lower than 2.5.

- in the whole range between zero and trip speed, when the vibration amplitude at probe location reaches the limit value A_{max}, the amplitude at any seal location shall remain lower than 75% of the allowable clearance.

The idea is that, if lower vibration amplitude can be ensured, it is possible to extend above 2.5 the amplification factor limit for Separation Margin requirement. A quantitative criterion can be derived by applying the same relation of inverse proportionality between AF and ζ reported in Equation (2). Therefore, for the responses to unbalances calculated in case A and B, the following acceptance criteria on AF and SM are proposed:

- for a critical speed peak with AF = k<2.5, standard API617 criteria are applicable. No SM from operating range is required; in the range between zero and trip speed, when the vibration amplitude at probe location reaches the limit value A_{max}, the amplitude at any seal location shall remain lower than 75% of the allowable clearance.
- for a critical speed peak with AF = k≥2.5, no SM is required if in the whole range between zero and trip speed, when the vibration amplitude at probe location reaches the limit value A_{max}, the amplitude at any seal location remains lower than (2.5/k)*75% of the allowable clearance (See *Figure 19*).

This means that, for example, in order to accept AF=3.5 in the operating speed range, the rotordynamic calculation should assess that vibration amplitude at any seal location is lower than 53% of the respective clearance.

In addition a check versus unbalance sensitivity can be introduced, in order to evaluate the vibration amplitude in absolute terms rather than in comparison with acceptance limit A_{max}. The rotor shall be unbalanced to excite 1st mode as per API617 2.6.2.7, and the calculated vibration amplitude at seal locations shall be still lower than (2.5/k)*75% of the allowable clearance.

If the calculated rotor response fails to meet either of these two criteria, then a Separation Margin between the critical speed peak and the operating range is still required, as per standard API617 criteria. The case of abradable seals, shall be treated on a case-by-case basis according to para 2.6.2.12 of API617.

Figure 19. Limit value for Amplification Factor as a function of damping ratio ζ. Points below the curve are acceptable regardless of the Separation Margin value. For points above the curve, the minimum required Separation Margin shall be calculated according to standard API617 criteria. The plot is limited to AF=5 since cases with larger values in AF of high pressure compressors in loaded conditions are very unlikely to occur.

CONCLUSIONS

The rotor response to unbalance for a centrifugal compressor equipped with honeycomb seal was calculated according to API617 prescriptions, and then recalculated including the aerodynamic coefficients (stiffness and damping) associated to the honeycomb seal. A comparison between the two sets of results show that the presence of the honeycomb causes 1) an upward frequency shift of the critical speed peak, 2) possibly a reduction of its amplification factor and 3) a reduction of the peak amplitude at most of the rotor stations, particularly in proximity of rotor midspan. These effects, experimentally observed, are more relevant for high pressure compressors and for honeycomb seals located close to rotor midspan.

The current calculation procedure and acceptance criteria for rotor response to unbalance are not optimized to assess the design of a high pressure compressor in presence of honeycomb seal. A calculation procedure able to include the effect of the honeycomb is presented, together with a proposed extension to the standard requirements for amplification factor and separation margin of critical speed peaks; the primary scope is to ensure a safe rotordynamic behavior under all operating conditions, while avoiding the application of unnecessary or biased constraints that may prevent the optimization of compressor design.

NOMENCLATURE

AF	Amplification Factor
CSn	nth Critical Speed
DE	Drive End (side)
FPU	Full Pressure Unbalance
MCS	Maximum Continuous Speed
NDE	Non-Drive End (side)
SM	Separation Factor
SOP	Settling Out Pressure

A	Vibration amplitude [μm]
f	Frequency [cpm]
F_0	Modulus of periodic exciting force [N]
C	Direct Damping [N s/m]
c	Cross coupling Damping [N s/m]
K	Direct Stiffness [N/m]
k	Cross Coupling Stiffness or generic stiffness [N/m]
N	Maximum continuous speed [rpm] or generic speed [rpm]
p	Bearing static load [N]
U	Unbalance [g mm]
W	Rotor weight [kg]
X	Displacement [m]
c_s	Damping coefficient [Ns/m]
m	Mass [kg]
δ	Logarithmic decrement
ω_n	nth natural frequency of the system [rad/s]
ζ	Damping ratio

Subscripts

FL	Full load condition
NL	No load condition
HC	Honeycomb
i	Iteration index
x	horizontal axis
y	vertical axis

REFERENCES

API 617, 2002, Axial and Centrifugal Compressors and Expander-Compressors for Petroleum, Chemical and Gas Industry Services, Seventh Edition, American Petroleum Institute, Washington, D.C.

API 684, 2005, API Standard Paragraphs Rotordynamic Tutorial: Lateral Critical Speeds, Unbalance Response, Stability, Train Torsionals, and Rotor Balancing, Second Edition, American Petroleum Institute, Washington, D.C.

Benckert, H., and Wachter, J., 1980, "Flow Induced Spring Coefficients of Labyrinth Seals for Applications in Turbomachinery," NASA CP 2133, Proceedings from a Workshop on Rotordynamic Instability Problems in High-Performance Turbomachinery - 1980, held at Texas A&M University, College Station, TX, pp. 189-212.

Childs, D. W., 1983, "Finite-Length Solutions for Rotordynamic Coefficients of Turbulent Annular Seals," ASME J. of Lubrication Technology, 105, pp. 437-445.

Childs, D. W. and Elrod, D., and Hale, K., 1989, "Annular Honeycomb Seals: Test Results for Leakage and Rotordynamic Coefficients; Comparisons to Labyrinth and Smooth Configurations," ASME J. of Tribology, 111, pp. 293-301.

Childs, D. W. and Wade, J., 2004, "Rotordynamic-Coefficient and Leakage Characteristics for Hole-Pattern-Stator Annular Gas Seals-Measurements Versus Predictions," ASME J. of Tribology, 126, pp. 326-333.

Fulton, J. and Baldassarre, L., 2007, "Rotor bearing loads with honeycomb seals and volute forces in reinjection compressors", Proceedings of the 36th Turbomachinery Symposium, Turbomachinery Laboratory, Texas A&M University, College Station, Texas, pp. 11 to 54.

Gelin, A., Pugnet, J. -M., Bolusset, D., and Friez, P., 1997, "Experience in Full-Load Testing of Natural Gas Centrifugal Compressors for Rotordynamics Improvements," ASME J. of Engineering for Gas Turbines and Power, 119, pp. 934-941.

Kleynhans, G., and Childs, D., 1997, "The Acoustic Influence of Cell Depth on the Rotordynamic Characteristics of Smooth Rotor/ Honeycomb Stator Annular Gas Seals", ASME Journal of Engineering for Gas Turbines and Power, Vol. 119, pp. 949-957.

Memmott, E. A., 1994, "Stability of a High Pressure Centrifugal Compressor Through Application of Shunt Holes and a Honeycomb Labyrinth," Proceedings of the Thirtieth Machinery Dynamics Seminar, CMVA, Toronto, Canada, pp. 211-233.

Nelson, C., 1984, "Analysis for Leakage and Rotordynamic Coefficients of Surface-Roughened Tapered Annular Gas Seals," ASME J. of Engineering for Gas Turbine and Power, 106, pp. 927-934.

Nicholas, J. C., 1989, "Operating turbomachinery on or near the second critical speed in accordance with API specifications", Proceedings of the 18th Turbomachinery Symposium, Turbomachinery Laboratory, Texas A&M University College Station, Texas, pp. 47 to 54.

Nielsen, K. K., Jonk, K., Underbakke, H., "Hole-Pattern and Honeycomb Seal Rotordynamic Forces: Validation of CFD-Based Prediction Techniques", Journal of Engineering for Gas Turbines and Power, Dec. 2012, Vol 134, ASME.

Smalley, A. J., Camatti, M., Childs, D., Hollingsworth, J., Vannini, G., and Carter, J., 2003, "Dynamic Characteristics of the Diverging-Taper Honeycomb-Stator Seal", paper GT2004-53084, ASME IGTI Conference, Vienna, Austria, June 2004.

Vannini, G., Cioncolini S., Calicchio V., Tedone F., 2011, "Development of an Ultra-High pressure rotordynamic test rig for centrifugal compressors internal seals characterization", Proceedings of the 40th Turbomachinery Symposium, Turbomachinery Laboratory, Texas A&M University, College Station, Texas, pp.46-59.

Weatherwax, M., Childs, D. W., "Theory Versus Experiment for the Rotordynamic Characteristics of a High Pressure Honeycomb Annular Gas Seal at Eccentric Positions", Journal of Tribology, April 2003, Vol. 125, ASME.

Weatherwax, M., and Childs, D.W., 2002, "The Influence of Eccentricity Effects on the Rotordynamic Coefficients of a High-Pressure Honeycomb Annular Gas Seal, Measurements Versus Predictions," ASME Paper 2002-TRIB-207

Zeidan, F., Perez, R., and Stephenson, E., 1993, "The Use of Honeycomb Seals in Stabilizing Two Centrifugal Compressors," Proceedings of the Twenty-Second Turbomachinery Symposium, College Station, TX, pp. 3-15.

ACKNOWLEDGEMENTS

The Authors would like to acknowledge Alberto Guglielmo and Davide Vagelli of GE Oil&Gas Company for their help in managing the experimental data, and Carmelo Mirmina for producing the compressor's cross section pictures.

A special thanks to Massimo Camatti of GE Oil&Gas Company for his suggestions to improve the overall quality of the paper.